11th Quarterly Progress Report
April 1, 2005 to June 30, 2005

Neural Prosthesis Program Contract N01-DC-02-1006

The Neurophysiological Effects of Simulated Auditory Prosthesis Stimulation: Summary of Electrode Configuration Effects Using the UCSF Guinea Pig Electrode

Submitted by:
Russell Snyder, Ph.D. [1]
John C. Middlebrooks, Ph.D.[2]
Alex Hetherington, M.S. [1]
Steve Rebscher, M.A.[1]
Ben Bonham, Ph.D.[1]

[1]**University of California, San Francisco**
Department of Otolaryngology – Head and Neck Surgery
Epstein Hearing Research Laboratory
533 Parnassus Avenue, Room U490E
San Francisco, CA 94143-0526

[2]**Kresge Hearing Research Institute**
University of Michigan
1301 East Ann St
Ann Arbor, Michigan

This report describes our progress during the 11th quarter of contract NIH-NIDCD-DC-02-1006 (April 1, 2006 - June 30, 2006). The bulk of this report describes a completed series of experiments that compares the spread of activation resulting from electrical stimulation of the cochlea in several configurations. Stimulating configurations included monopolar, bipolar, and tripolar configurations with varying separations between stimulating electrodes of the UCSF guinea pig implant. Other work completed during the quarter is briefly described in the following section.

Work completed during quarter

During the previous quarter, we have completed one cat and sixteen guinea pig physiology experiments. These experiments were designed to investigate several aspects of responses to acoustic and electrical stimulation, including:

- Interactions between two interleaved pulse trains presented on one and two cochlear implant channels.
- Comparison of the spread of activation using UCSF-type electrodes, of activation using a Nucleus banded animal implant, and of activation using visually placed Pt/Ir ball electrodes. The UCSF electrode is designed to be space-filling within the scala tympani, while the Nucleus electrode is not. The results of these experiments indicate very significant differences in spatial specificity of stimulation between the UCSF and Nucleus electrodes. This study will compare the spread of activation using these electrodes with spread of activation during noise band stimulation. Results of these experiments will be directly comparable with published data of Frijns et al., which modeled activation due to point sources of varying longitudinal separation in guinea pigs. We are currently analyzing the data from these experiments, and will report the results of our analyses in a future QPR.
- Pulse trains of rates varying between 20 and 2560 pulses per second.
- Sinusoidally amplitude modulated pulse trains with carrier rates of 250 and 1000 pps. In these experiments, amplitude modulation was varied from 10 - 200 Hz, modulation depth was 100%, and three levels of modulation depth between threshold and threshold+6dB were used.
- Responses to two tones presented simultaneously. These experiments comprise a model in a normal-hearing animal for responses to electrical pulse trains presented on two interleaved channels. These experiments will be followed by further studies using two sinusoidally amplitude modulated (SAM) tones that covary in amplitude.
- Effects of bipolar and tripolar electrode separation.

We have also completed our first experiment using a 32-channel probe from NeuroNexus. This experiment was carried out in a cat, and included recording responses to acoustic stimulation. Figures from this experiment will be included in the next QPR.

Several of these experiments were conducted in collaboration with John Middlebrooks. These experiments complete acquisition of data for our electrical forward masking experiments using unmodulated pulse trains as maskers and probes.

In addition to the physiology experiments described above, we have also made progress in other areas:

- Enhancements to experiment software and hardware
    - We have modified our experiment software to allow it to control our new Tucker-Davis Technologies RX-8 multi-channel D/A converter. Since the multiple TDT RP2 processors we have been using do not have synchronized internal clocks, we could independently address at most two phase locked analog signals (or four non-phase locked signals, when using two RP2s). The RX8 hardware we will allow us to independently control up to twelve independent phase-locked channels. This ability is required for stimulation of multiple implant electrodes in our planned experiments using electrical speech stimulation.
    - We have generated software to generate and calibrate acoustic noise bands. Representative spectra of several noise bands generated by this software are included below in this report. Our on-line analysis software has also been modified to accomodate experiments using stimulation with these noise bands

- Electrode fabrication
    - We have fabricated five guinea pig implant electrodes.
    - We have fabricated four pairs of Pt/Ir ball and wire electrodes for use in experiments using visually-placed balls.
    - We have replaced our worn-out guinea pig implant mold with a new mold.

- We have conducted an experiment to compare non-physiological "background noise" recorded during stimulation using the Ellinger multi-channel stimulator (described in a previous QPR) with background noise recorded during stimulation using our high-voltage analog switch (described in QPR#3). The results of these experiments will be included in our next QPR.
- We have begun acquiring data for a morphology study that will compare response profiles predicted using longitudinal and radial electrode positions and theoretical models with response profiles recorded during electrical stimulation.
- We have begun analysis of data from the experiments described above, as well as continued analysis of data obtained during previous experiments.

Travel

- J. Middlebrooks traveled to UCSF to conduct guinea pig experiments.
- B. Bonham traveled to the University of Michigan to evaluate a TDT 32-channel recording system in the lab of J. Middlebrooks. This travel was not charged to this contract.
- R. Snyder traveled to the University of Michigan to conduct guinea pig experiments. This travel was not charged to this contract.

SUMMARY OF THE EFFECTS OF ELECTRODE CONFIGURATIONS USING THE UCSF GUINEA PIG ELECTRODE

Introduction

Clinically applied cochlear implants are highly successful prosthetic devices. And, although there several types of implants, they all consist of a receiver, a processor/stimulator and an intracochlear electrode array. In these studies we have concentrated on the consequences of different electrode designs. There are at least 5 different commercial intracochlear arrays, which vary significantly in their design. However, all of these arrays are designed to be inserted into the scala tympani of deaf human subjects. The performance of these electrodes varies dramatically for subject to subject and the factors that influence electrode performances are poorly understood,. In our attempts to begin to understand these factors and to simulate auditory prosthesis (AP) stimulation, we have undertaken three approaches. First, we have examined the effects of intracochlear stimulation of animal using human intracochlear electrode arrays. Thus, we have inserted human intracochlear arrays into the scala tympani of guinea pigs and recorded the neural responses that are evoked. Although this approach is a direct one in that it allows us to examine the physiological effects of stimulation with a human electrode, the human electrode arrays do not fit the guinea pig scala tympani in the same way that they fit in the human scala. The guinea pig scala tympani, for example, is smaller in diameter, has a tighter radius of curvature and a greater basal to apical pitch than the human scala. Thus the electrode contacts of the human array may adopt different positions with the guinea pig scala than in the human scala relative to the neural elements and the effects of stimulation may not be comparable.

Therefore, we have pursued a second approach in parallel with the first. We designed and fabricated an intracochlear electrode that is engineered specifically to fit into the guinea pig scala (see QPR #1, 2 and 3 for this contract). The carrier of this electrode is designed to fill the scala tympani and therefore, to place the stimulating contacts of the array in close proximity to the excitable neural elements along its entire length In contrast, the human array does this only at its most apical sites when it is inserted into either the human or the guinea pig scala.

Finally, although these intracochlear electrode arrays model those used in humans, they have several disadvantages as experimental tools. Among these disadvantages are: They are limited in the range of stimulation configurations that can be employed with them. For example, they do not allow (in the case of the human arrays) or easily allow (in the case of the guinea pig array) exploration of the effects of stimulation using radial configurations. The human array allows bipolar and tripolar stimulation using only contacts array longitudinally along the cochlear spiral. Nor do they allow electrode separations or positions to be varied continuously.

In addition to these limitations, they are limited in the ease with which the details of electrode position can be directly documented. For example, the degree of juxtaposition of the contacts to the osseous spiral lamina is not possible. The carrier obscures or blocks the visual determination of the anatomical relationship between electrode contacts and anatomical features of the cochlea. For example, it is not possible to determine the exact radial position of the contacts. Are they closer to the habenula or closer to Rosenthal's canal? Are they juxtaposed to the osseous spiral lamina or to the spiral ligament? Therefore, we have pursued in parallel a third approach: the use of visually placed ball (VP ball) electrodes. These electrodes consist of insulated wires that terminate in bare metal spheres. The spheres approximate the size of the contacts used in the guinea pig array, but they can be individually placed in precise arbitrary locations and these locations can be controlled and documented visually.

In this report, we will document the effects that some configuration variables have on threshold, the spread of excitation across the tonotopic organization of the inferior colliculus and the single-channel interactions between excitation patterns evoked by each member of a pair of

electrodes in different configurations. We focus on our guinea pig electrode, since such documentation is required background for our subsequent presentations of two- and multi-channel interactions using these electrodes. One particular focus is on the effects of longitudinal separation between intracochlear electrode contacts, since, although this variable has been modeled in computer simulations (see Briaire and Frijns, 2000; Briaire and Frijns, 1996; Frijns et al, 1995) and is commonly employed in clinical application of cochlear implants, no physiological confirmation or examination of the effects of longitudinal separation between contacts have been published. In addition, we will document the differences between the three stimulation configurations (monopolar, bipolar and tripolar) to simulation of AP stimulation. We are interested in these variables and the differences between stimulation approaches, because we believe that a better understanding the factors that influence threshold, spread of excitation (frequency selectivity) and dynamic range will contribute of better implant stimulation schemes that will provide stimulation at lower thresholds, greater spatial (frequency) selectivity and less channel interaction.

Methods

All procedures were carried out under a protocol approved by the IACUC at the University of California. All surgical, general recording, signal generation, and data analysis procedures have been described previously (see QPR# 6), therefore, they will be described only briefly here.

All procedures were carried out under an approved protocol at the University of California at San Francisco. Guinea pigs were pre-anesthetized by an IM injection of ketamine/xylazine (4:1). Further IM injections of ketamine/xylazine were used to maintain an areflexic state of anesthesia. Three EKG silver wire recording leads were inserted subcutaneously and allowed heart rate and respiratory rate to be monitored throughout surgery and during the subsequent experiment. An additional silver wire, which served as a recording ground was inserted subcutaneously at the nape of the neck. A rectal probe and temperature-controlled water blanket were used to record and maintain normal core body temperature. A tube was inserted into the trachea to maintain a patent airway. The head was shaved and the scalp was incised down the midline and the tissue overlying the bone was retracted. Two or three bone screws were inserted into the top of the skull and covered with dental acrylic. A large bolt for holding and stabilizing head was fixed to the skull between the screws with more dental acrylic. The bolt was secured in a flexible arm (Noga). The scalp behind each ear was incised and reflected to expose both ear canals, which were sectioned to allow insertion of hollow stereotaxic ear bars. The right tympanic membrane was perforated, the right middle ear bones were disarticulated and the right ear canal was filled with dental acrylic. This effectively deafened the right ear. In addition, in some cases, the right cochlear was destroyed in addition using a dental burr after the middle ear bones were disarticulated. This addition step had noticeable effect on the ipsilateral ICC responses to contralateral cochlear stimulation so it was omitted in subsequent experiments.

The temporalis muscle over the right side of the calvarium was reflected and the calvarium exposed. The parietal bone anterior to the transverse sinus was thinned with a dental burr and small rongeur was used to remove the bone and expose the dura overlying the right occipital cortex. A silver wire was inserted between the parietal bone and the dura and fixed in place to serve as a reference for recording probes or tungsten microelectrodes. The dura was excised and a hole in the lateral occipital cortex posterior the posterior horn of the lateral ventricle was aspirated to expose the dorsolateral surface of the inferior colliculus.

The animal was then placed into a Kopf stereotaxic head holder and a micromanipulator was used to insert multi-channel recording, 16-channel single-shank silicon recording probes

(CNCT University of Michigan). The probes had iridium-coated recording sites spaced linearly at 100 micron increments. Prior to insertion, probe sites were immersed in distilled water cleaned by passing anodic and cathodic current through each site until obvious bubbles of oxygen or hydrogen appeared. After cleaning, site impedances were typically 300 kOhms. The recording probes were inserted into a custom-built headstage, which was held by a micromanipulator. Using the micromanipulator, the probes were inserted into the IC along a standard trajectory that was in the coronal plane at an angle of 45 º off the sagittal plane. While the probe was being inserted, responses were recorded from each recording site to tone bursts over a range of frequencies and intensities. The probe penetration depth was adjusted until probe-site CFs spanned a range of frequencies from 3 kHz to approximately 25 kHz and the CFs were arrayed monotonically from low frequencies superficially to high frequencies deep in the IC. This effectively calibrated the recording probes and ensured that recordings were made from the central nucleus rather than the external nucleus, since the tonotopic gradient reverses at the boundary between these two structures.

To stabilize the calibrated recording probes, a 1% solution of warm liquid agarose was injected into the space formerly occupied by the occipital cortex to cover the exposed nervous tissue. The agarose was allowed to solidify and then the dorsal surface of the agarose, the bone of the calvarium and the distal portion of the probe PC board was covered with dental acrylic. When the acrylic polymerized, the opening in the skull was effectively sealed and the probe was fixed in place. Once the recording probe was fixed in place, the headstage could be removed from the recording probe, the ear bars could be removed and the animal could be removed from the stereotaxic holder. The animal was rotated to allow access to the left cochlea and a calibrating ear bar was inserted into the left ear canal.

Sound stimuli were digitally generated (TDT System III), amplified (using a Samson audio amplifier) and presented by Radio Shack Super-tweeters attached to custom ear bars that were inserted into the left ear canal. Sound levels were calibrated using a probe microphone (B&K ½" microphone, model 4182) with the tip of the microphone placed through the ear bar near the tympanic membrane. The calibrated acoustic signal was adjusted so that tone transfer function at the ear canal was flat within +/- 2dB over the range between 2 kHz and 41.5 kHz.

Recording: Neural signals from recording probes were passed through a headstage, amplified using a custom-built preamplifier and post-amplifier and bandpass filtered (100 – 6000 Hz). The amplified and filtered signals were digitized and sampled at 20 S/sec/channel (National Instruments, model 6071E). Experiment control, stimulus generation, data acquisition, data analysis and display were carried out using custom software (LabView/Matlab). Multi-unit activity was recorded with 16 channel probes. Spike times were determined in real time as threshold-crossing times using custom software. A neuronal waveform was required to cross and then return across a threshold voltage within a preset amount of time (usually 0.4 ms) in order to be counted as a spike. This prevented low frequency evoked (or volume conducted) potentials from being counted as a spike. Thresholds for each electrode were determined independently by computing the RMS amplitude of a 90 ms sample of spontaneous activity on each electrode immediately prior to recording a response area, then multiplying that value by a constant (usually between 2.5 and 3.5 RMS). In most, but not all, cases, activity recorded on electrodes on the multi-channel probes were clearly multi-unit, and could not be resolved by spike sorting into single units. For single-unit activity recorded either with the multi-channel probes or with high-impedance tungsten electrodes, a similar procedure was followed. For these recordings, we observed what appeared to be spike

activity from a single neuron that was far above the RMS background level. Similar means were used to identify spike times for these recordings.

Following a series of "acoustic calibration" recordings, in which frequency response maps were recorded at each of the fixed recording probe sites, the round window of the left cochlea was exposed and left cochlea was deafened with a 50 – 100 μL injection of 10% Neomycin sulfate. Following deafening, one of three different types intracochlear stimulating electrodes were inserted into the cochlea and the responses evoked by activation of different channels in different configurations of each electrode were recorded. In most cases, the first electrode was a UCSF guinea pig electrode (see QPR#2, 3, 8), followed by a nucleus banded electrode; followed by visually placed ball electrodes.

Symmetric biphasic current pulses were used for stimulation. One intracochlear electrode, E_n, was chosen to be designated the "active" electrode. For stimulation in the monopolar configuration, activating current was applied to the active electrode, E_n, and an extracochlear electrode served as the path for all the return current. The monopolar configuration is abbreviated in this report as nM (e.g., 3M when intracochlear contact #3 served as the active contact). For stimulation in the bipolar configuration, the activating current was applied to one intracochlear electrode E_n and another intracochlear electrode E_{n+1} provided the return current path. If the active electrode was contact #3 and the return contact was electrode #4, the stimulation configuration would be abbreviated configuration 3,4. The series of such adjacent bipolar configurations are designated generally as BP+0 configurations. If the active and return electrodes were separated by one electrode site $E_{n\ \text{active and}}\ E_{n+2\ \text{retlurn}}$, e.g., electrodes #3 as the active and #5 as the return, this would be abbreviated 3,5. Such configurations are designated generally as BP+1 configuration, if n electrodes intervene between the active and the return electrodes; they are designated BP+n. In the tripolar configuration, activating current was applied to E_n, and half that current was applied in the opposite polarity to each of the two adjacent electrodes, E_{n-1} and E_{n+1}. In this configuration, all the return current flows through electrodes E_{n-1} and E_{n+1}, which are adjacent apical and basal electrodes, respectively, to the active electrode E_n. The tripolar stimulation is abbreviated in this report as <n-1,n,n+1> (e.g., <2,3,4> when intracochlear contact #3 served at the active and the adjacent contacts, #2 & #4, served as the return contacts). Such configurations are designated generally as TP+0. If there is an electrode intervening between the active and return electrodes, these configurations are designated TP+1; if two electrodes intervene, these configurations are collectively designated TP+2.

In each experimental series, for each "active" electrode, a single current pulses or train of current pulses were presented in 1 or 2 dB increments in intensity over a range of intensities, from below minimum threshold up to a maximum of 1.6 mA. Responses of neurons clusters near the sixteen recording sites were amplified and digitized, and spike times were identified during on-line analysis. Digitized waveforms were also stored for later off-line analysis.

The minimum response latency for ICc neurons is approximately 5 ms, while latencies can be as long as 25 ms following a single current pulse. Single pulses or pulse trains were used to compose families of spatial tuning curves (STCs) for each stimulus configuration and intensity. The STC abscissa is stimulus intensity, and the ordinate is IC depth or recording site number. The strength of the neural response is encoded by color.

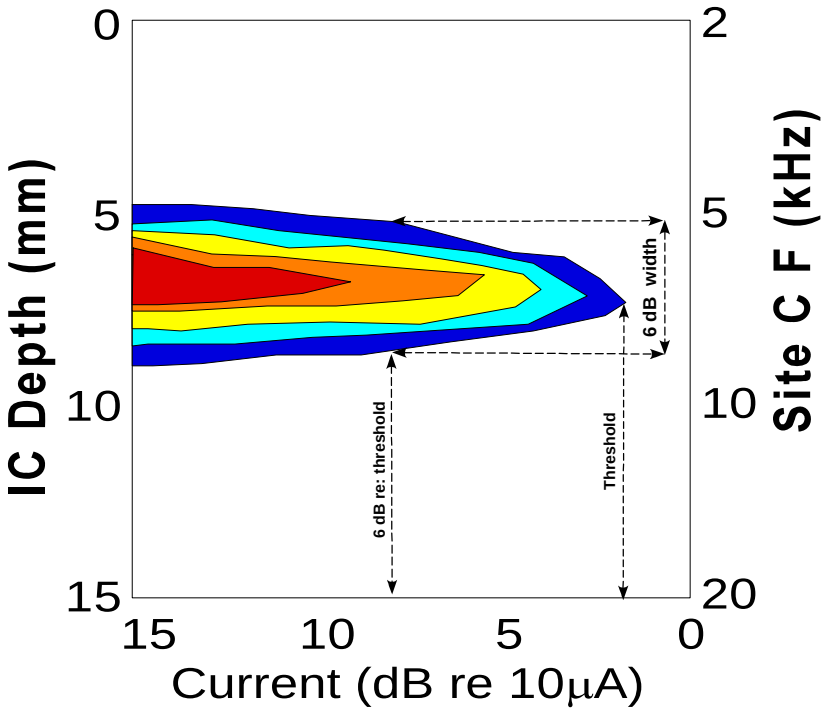

Figure 1. Calculation of threshold and 6 dB width of an electrically evoked STC.

From each STC, rate/level curves for each electrode were computed. For each recording site, the saturation rate was visually estimated and was recorded. Spontaneous response rate at each site was estimated by the average response during the 10 ms stimulus-free periods preceding each current pulse or pulse train. Minimum threshold at each site was identified as the stimulus level inducing a spike rate that exceeded the spontaneous rate by 25% of the difference between spontaneous and saturation rates. The overall minimum threshold was the lowest threshold among the sixteen recording sites. The dynamic range of a site was determined by taking the difference in stimulus levels that produced response rates of 10% and 90% of the difference between threshold and saturation levels.

Spatial tuning curves were normalized before determination of width. To normalize each STC, the spontaneous rate (number of spikes) was subtracted from the raw response rate on each electrode, and that value was divided by the difference between the saturation rate and the spontaneous rate. So, response rates of the normalized STCs loosely ranged between 0 and 1. From the normalized STCs, iso-rate contours were computed. The "width" of each spatial tuning curve was determined at a stimulus level 6 dB above the overall minimum threshold, and was computed as the distance from the deepest to the most superficial recording sites whose normalized response rates exceeded 0.3, Figure 1. A large number of spatial tuning curves were too broad to measure widths at stimulus levels greater than 6 dB above threshold. In these cases the STC width was estimated as 1600 microns, i.e., the entire length of the recording probe.

Results and Discussion

At the beginning of each experiment the cochlea is stimulated acoustically with a series of tones and the responses to these tones are assembled in frequency response maps (see Figure 1A).

Using these maps, the characteristic frequency of each recording site is estimated. In addition, by re-plotting the data, acoustically evoked spatial tuning curves (STCs) can be constructed. Figure 2 illustrates the same data in Figure 1A re-plotted as

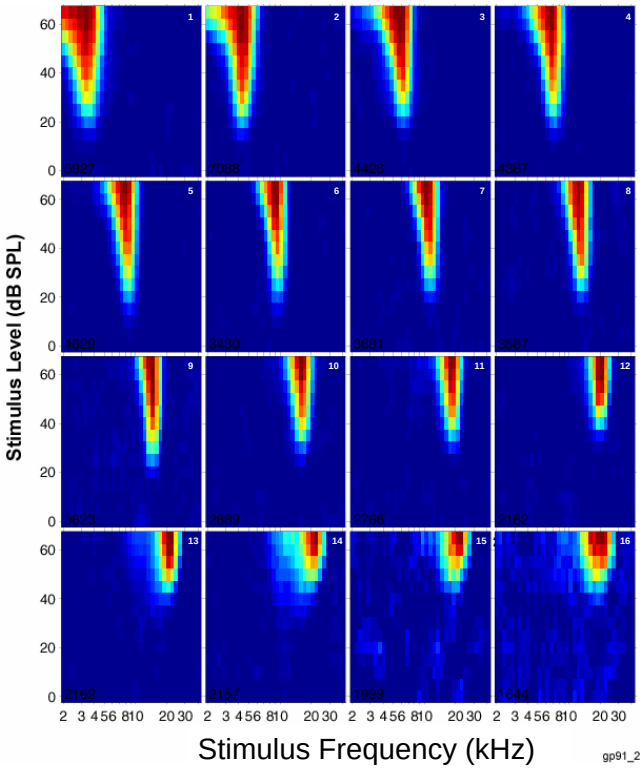

Figure 1A. Acoustic frequency response maps from GP91. Each panel represents a multi-unit frequency response map in the right ICC evoked at one site (indicated in the upper right) of a 16 site, single shank recording probe. The sites are numbered with "1" indicating the most proximal and "16" indicating the most distal. The frequencies of contralaterally presented tones are plotted along the abscissa of each panel and their intensity along the ordinate. Within a panel, each facet represents the color-coded response amplitude at that site to the corresponding frequency intensity combination. The color code is red for the maximum evoked activity and dark blue for spontaneous activity.

spatial tuning curves (STCs). These representations are useful for the purposes of this discussion, since they allow acoustic and electric responses to be easily and directly compared. The acoustically- evoked STC produced by varying the intensity of a 10.4 kHz tone in Figure 2, for example, can be directly compared with an electriccaly- evoked STC produced by varying the stimulus intensity of an electrode located at the 10.4 kHz place in the guinea pig cochlea. They also allow stimuli that differ in bandwidth to be compared. These acoustic tone-evoked STCs are narrowly tuned and display an orderly and progressive shift from shallower to deeper ICC locations of their minimum threshold as the tone frequency progresses from lower to higher frequencies. An ideal intracochlear electrode might have 32 such sites linearly arrayed along the cochlear spiral, each of which evokes an STC that is comparable to these STCs.

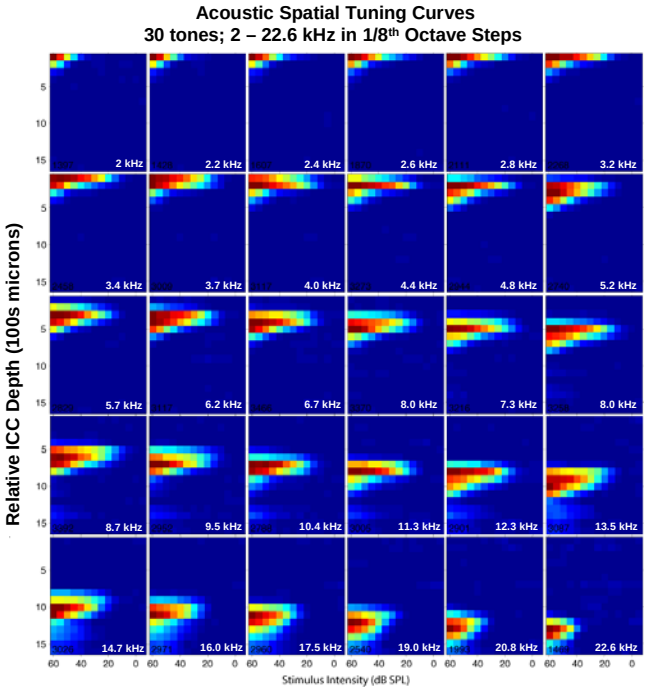

GP91_2

Figure 2. Acoustic tone-evoked spatial tuning curves (STCs). These STCs are constructed using the same data illustrated in Figure 1. Each panel represents the activity evoked by a different frequency tone. Tone frequency is indicated in the lower left corner of the panel. Tone intensity in dB SPL is plotted on the abscissa and relative ICC depth in 100s of microns (probe site number) is plotted on the ordinate. The activity evoked by the lowest frequency tone is illustrated in the upper left and that evoked by the highest frequency tone is illustrated on the lower right.

Although most electrically evoked activity is not as narrowly tuned as acoustic tones, most acoustic signals are not pure tones. Therefore, we have begun to stimulate guinea pig cochleas with wider band signals and to compare the evoked responses with those observed following electric stimuli. We have stimulated the cochlea with noise bands of varying center frequencies and bandwidths and analyzed the evoked responses. Figure 3 illustrates the power spectra of 5 noise bands. These bands are all ½ octave wide, but they vary in center frequency from 2.5 kHz to 25 kHz. They were generated so that their peak amplitudes are approximately equal within and between bands. Stimulation using noise bands such of these have been used to simulate intracochlear stimulation, so called vocoder noise simulation of cochlear implant stimulation. They have also been used to simulate stimulation with different electrodes configurations that differ in their spatial spread.

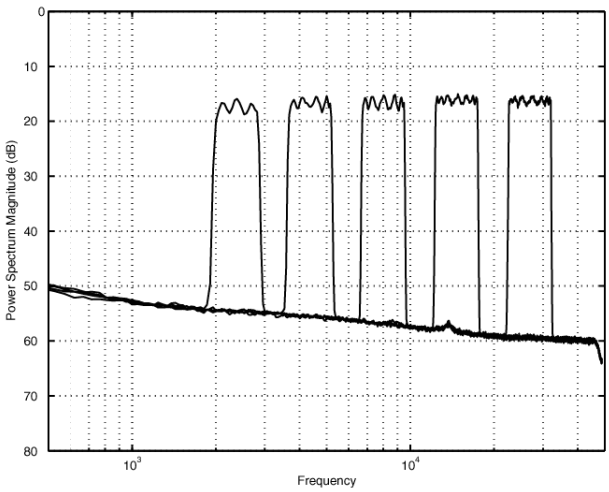

Figure 3. Power spectra in dB of five ½ octave noise bands recorded using a calibration microphone. The illustrated noise floor is the noise floor of the B&K calibration microphone.

In Figures 4 and 5 the results of stimulation with two noise band series are presented. The bands in these series differ in their center frequencies, but their bandwidths and overall intensities are varied over the same range. In each of these STC series, a center frequency was chosen and then bandwidth was varied from 1/8th octave to 2 octaves in 1/8th octave steps and in intensity was varied from 80 to 20 dB attenuation in 5 dB steps.

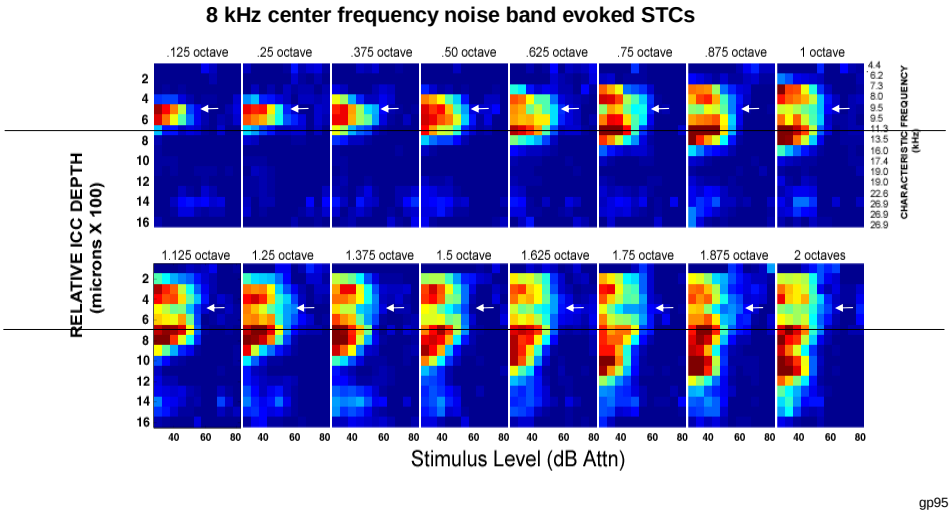

Figure 4. STCs evoked by stimulation using noise bands that have a center frequency of 8 kHz and vary in bandwidth from 1/8 octave (upper left) to 2 octaves (lower right) in 1/8 octave steps. The bandwidth is indicated at the top of each STC. The characteristic frequency (CF) of each site, estimated from the tone evoked responses, is indicated to the left of the top row. Activity evoked on site #5, tuned to 9.6 kHz the center frequency of the noise bans, is indicated by the arrows, activity on site #7, tuned to 11.3 kHz, is indicated by the thin black line.

Figure 4 illustrates the STCs evoked by progressively wider noise bands with a constant geometric center frequency of 8 kHz. As can be seen by scanning across these STCs, the bands with wider bandwidths evoke activity that is more broadly distributed across ICC depth. The narrowest band, an 1/8 octave wide (far left, top row), evokes activity that is centered on site #5, i.e., it evokes the highest activity at the lowest intensity at site #5 (indicated by the arrows). This site is tuned to approximately 9.5 kHz, slightly higher than the band's center frequency. Comparing this 1/8 octave noise STC with the tone STCs, illustrates that distribution is comparable to that evoked by an 8 kHz tone presented across a range of intensities from 0 to 40 dB SPL. At 50 dB attenuation, this noise evoked activity at two recording sites (#5 & 6). At 35 dB attenuation, it evoked activity at four sites (# 4 – 7). As noise bandwidth increased across the same attenuation range, evoked activity spread to adjacent sites and the activity at the most sensitive sites increased and were seen at lower stimulus levels. Spread of excitation was most rapid to deeper sites (higher frequencies) as the width of the noise bands increased. At many sites, e.g., #7, indicated by the horizontal black lines, evoked activity increased more or less monotonically and then saturated as bandwidth increased. At other sites (e.g., sites #5 and 6) activity increased then dramatically decreased.

Figure 5 illustrates STCs evoked in the same animal using noise bands with a higher center frequency, 12 kHz. These higher frequency bands evoke activity profiles that are deeper in the ICC. An 1/8 octave 12 kHz noise band (far left, top row) \activated sites that are sensitive to tones of approximately12 kHz, sites #7 and 8. These sites lie deeper in the ICC than the sites sensitive to

the 8 kHz bands shown in the previous figure. As in the previous figure, bands with wider bandwidths evoke activity that is more broadly distributed across the depth of the ICC. And just as in the previous figure, sites #7 & 8 have evoked activity that is a nearly monotonic function of

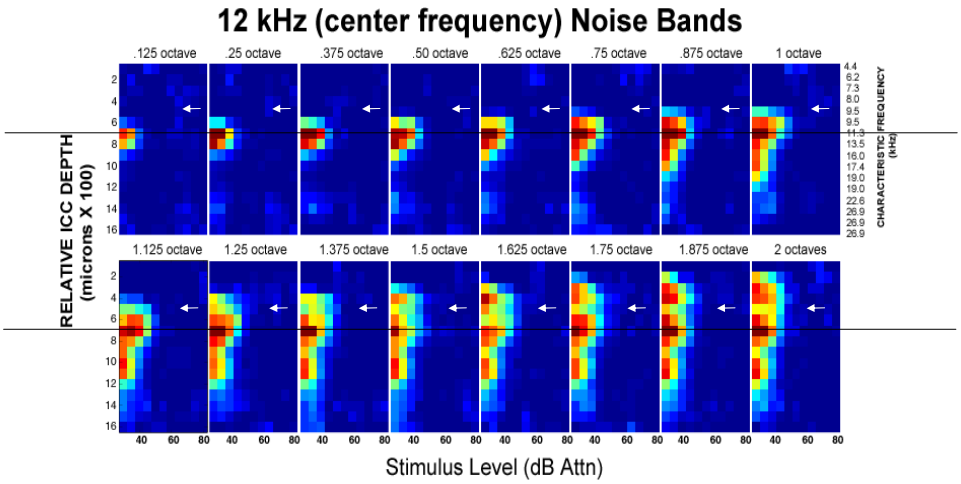

Figure 5. Spatial tuning curves evoked by 12kHz center frequency noise bands. These bands differ in bandwidth from 1/8 octave to 2 octaves. As in Figure 4A, the noise bandwidth is indicated at the top of each STC; the characteristic frequency (CF) of each site, estimated from the tone evoked responses, is indicated to the left of the top row. Activity evoked on site #5, tuned to 9.6 kHz, is indicated by the arrows, activity on site #7, tuned to 11.3 kHz, the approximate center frequency of the noise bands, is indicated by the thin black line.

bandwidth and, just as seen in the previous figure, the activity on site #5 (indicated by the arrows) is distinctly non-monotonic with increasing bandwidth. This suggests that the interactions between stimulus bandwidth, intensity and center frequency are at least partly site dependent.

The non-monotonic behavior of acoustically evoked response described above suggests that, as the bandwidth of many acoustic stimuli increases, the excitation patterns will not simply spread across the tonotopic organization of the IC. There will be complex interactions between stimulus intensity, stimulus center frequency and stimulus bandwidth. And these interactions may be site dependent, at least in part. Moreover, it also suggests that high fidelity reproductions of neural responses to broadband acoustic signals, such as speech and music, cannot be reproduced using electric stimuli which simply use electrode configurations that evoke broad excitation

Figure 6A. An image of the guinea pig electrode array used in these experiments. The array has 8 stimulating electrode contacts embedded in a silicone elastomer carrier. The sites are about 100 microns in diameter and have a center-to-center spacing of about 250 microns. Upon insertion, the round window will be located at approximately the red dashed line.

patterns. They must be reproduced by using multiple narrowband channels and activating these channels using sophisticated stimulus paradigms.

In order to explore how such narrowband channel might be constructed we have examined the effects of stimulation with narrowly spaced electrodes. One such electrode is illustrated in Figure 6A. This electrode consists of an array of 8 platinum wires each terminating in a spherical contact. The wires and contacts are embedded in a silicone elastomer carrier. The carrier is designed to be space-filling and to place the contacts in a longitudinal series along the osseous spiral lamina of the hook and basal first turn at a radial locations that are somewhere between the habenula and Rosenthal's canal.

The sites have a diameter of about 100 microns and a center-to-center spacing between sites of about 250 microns. The electrode is inserted into the scala tympani through an enlargement of the round window, shown in Figure 6B.

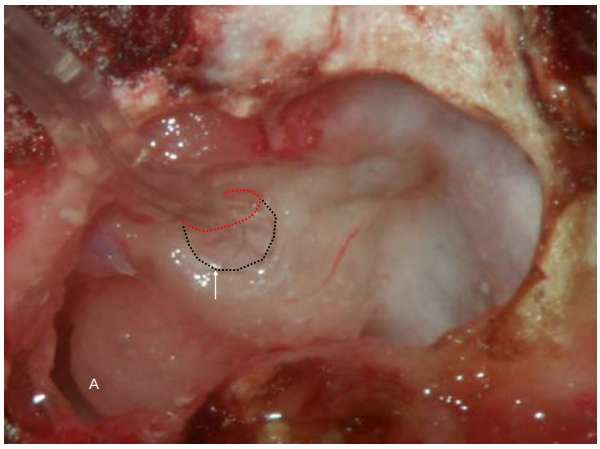

Figure 6B. An image of the guinea pig cochlea with the intracochlear electrode inserted. Before its enlargement, the rim of the round window would have been located at the dashed red line. The enlargement of the round window to accommodate the electrode carrier is indicated by the dashed black line. The apex of the cochlea is shown at "A". The top of the last (most basal) electrode contact (#8) is shown at the arrow.

Once the guinea pig electrode is inserted into the scala tympani, the contacts should lie in a linear array distributed along the cochlear spiral at the locations indicated by the blue circles illustrated in Figure 7. These electrode sites are numbered sequentially beginning with the apical-most site.

Figure 7. A cast of the guinea pig scala tympani illustrating the location of the array contacts after insertion. The numbered circles indicate the approximate location of each of the 8 stimulating contacts. The white arrows indicate the location of the basilar membrane. The red dashed line indicates the location of the round window.

The curves in Figure 8 illustrate several common properties of the activity patterns evoked by stimulation using our guinea pig electrode activated in three different configurations, monopolar

(upper row), adjacent bipolar (BP+0) and adjacent tripolar (TP+0). For example, all three configurations can evoke selective, tonotopically appropriate activity patterns in the ICC. These activity patterns are tonotopically appropriate in that activation of apical intracochlear contacts evoke activity at more superficial (lower frequency) ICC sites, whereas activation of successively more basal contacts evoke activity at deeper (higher frequency) sites. Thus, the left-most STC in the second row illustrates that activation of bipolar pair 1,2, the most apical bipolar electrode combination, evokes activity centered around site #7 (tuned to 11 kHz), whereas activation of the more basal pair 6,7 (next to last STC in the middle row) evokes activity centered around site #12, which is tuned to 20.7 kHz. Activation of the intermediate electrode pairs evoke activity at intermediate ICC locations which are tuned to intermediate frequencies. Tripolar stimulation (bottom row of STCs) also evokes highly selective tonotopically appropriate activation of the ICC. Although tripolar configurations often evoke activity that appear to be more selective than bipolar stimulation (compare, for example, the STCs evoked by activation of bipolar pair 2,3 with that evoked by tripole 2,3,4), these two configurations evoke nearly identical activation patterns (compare, the STCs evoked by bipolar pair 6,7 and tripole 6,7,8).

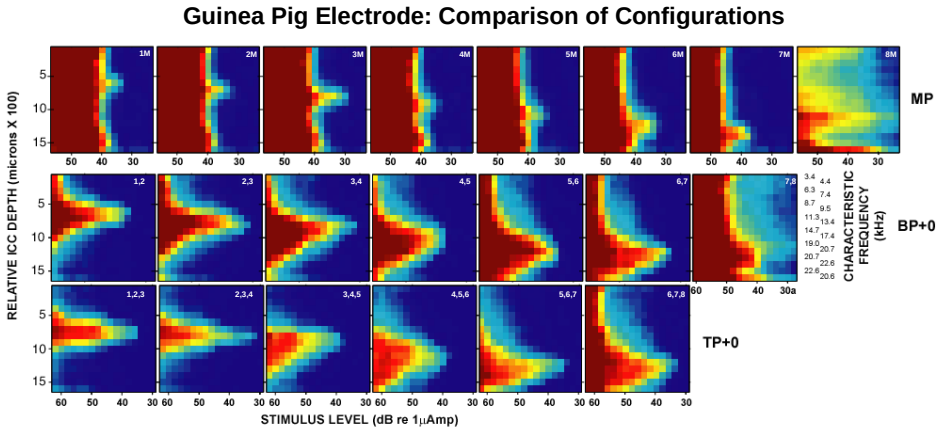

Figure 8. Spatial tuning curves (STCs) evoked by stimulation of the guinea pig electrode activated in three different configurations: monopolar (MP) in the upper row, adjacent bipolar (BP+0) in the middle row, and adjacent tripolar (TP+0) in the bottom row. The specific electrode combinations used to evoke activity in each STC are indicated in the upper right corner of the curve. Within each row curves are arranged such that the activity resulting from stimulation of the most apical electrode combination is on the far left and those from the more basal combinations are sequentially distributed to the right. The upper row of curves illustrates the effects of activation of all 8 MP combinations. The middle row of curves illustrates the effects of activation of all possible BP+0 combinations. The bottom row illustrates the activity patterns evoked by activation of all possible TP+0 configurations. Characteristic frequencies (CFs), estimated from acoustic stimulation prior to deafening and implantation, of each recording probe site is indicated to the right of the most basal bipolar STC. In this and all subsequent similar curves saturated activity is coded at dark red and spontaneous activity is coded as dark blue.

Using this electrode, even monopolar stimulation often can evoke selective and tonotopically appropriate activation at low stimulus levels. However, this tonotopically appropriate

activity is evoked only a stimulus levels near minimum threshold over a narrow range of stimulus levels. In Figure 8, for example, activation of electrode contact 1M, the most apical monopole, produces relatively selective activation of the ICC, which is centered at recording site #6 (tuned to 9.5 kHz) at levels between 34 and 38 dB. Stimulation of 2M produces activity that is centered on site #8, which is tuned to 13.4 kHz. Likewise, activation of contact 7M at levels near threshold evokes activity centered at the site #14 which is tuned to 23 kHz. With the exception of contact 8M, the most basal contact, activation of each successively more basal monopolar contacts, 1M to 7M, produced relatively selective activation at successively deeper (higher frequency) recording sites centered at sites, 6, 7, 8, 9.5, 11, 12.5, 14 respectively. However, at stimulus levels 6 – 8 dB above threshold, activity evoked by all these monopolar electrodes spreads broadly across the ICC encompassing the entire nucleus. This contrasts sharply with bipolar and tripolar stimulation in which selectivity extends across a broad range of intensities of 15 to 20 dB in most if not all animals. Thus, although selective monopolar stimulation is not universally observed, these data indicate that monopolar stimulation can evoke selective, tonotopically-appropriate activation in some animals at some (low) stimulus levels. We believe that this observation is important, since monopolar stimulation is the stimulus configuration most generally used in human cochlear implants. Moreover, variations in monopolar selectivity over very narrow dynamic ranges may account for a significant variation in cochlear implant performance.

Figure 9 illustrates the effects of systematically altering the separation between contacts of our guinea pig electrode. It illustrates the differences between STCs evoked by activation of adjacent bipolar pairs, BP+0, with those evoked by progressively more widely separated pairs, pairs that eventually span the full length of the electrode, BP+6. Although these data were collected in another animal, the STCs evoked by BP+0 stimulation can be compared to those seen in the previous figure. The patterns appear comparable. Stimulation of all the BP+0 pairs produce relatively selective, tonotopically appropriate excitation patterns in the ICC. However, as the separation between the contacts increases, the tonotopically-appropriate selectivity of stimulation decreases. This is a common observation and Figure 9 illustrates that this is due to several effects. In part, it is due to a loss in selectivity (a broadening of the STCS) as the separation between bipolar contacts increases. Scanning down any of 5 columns on the left of Figure 9, one can see a clear tendency for the STCs to become broader as contact separation increases, until the selectivity is as poor or poorer than the poorest monopolar activity patterns. In addition to broadening, there is a tendency for more widely separated, equally effective stimulation contracts to evoke responses two separate ICC populations, one associated with each constituent contact. The overlap and interaction of these two populations leads to a decrease in tonotopically appropriate selectivity. For example, in the 4 left-most STCs in the BP+2 row of STCs (third from the top), each electrode contact 1 & 4, 2 & 5, 3 & 6 and 4 & 7 appears to evoke an, at least partially, independent ICC response (white arrows), i.e., one appropriate for each constituent contact. Thus, the white arrows in these BP+2 STCs are approximately equally spaced (just as the contact pairs are equally spaced), and they shift down to higher frequencies ICC sites (just as the constituent contacts shift to more basal, higher frequency locations as one scans from left to right). Likewise, in the column involving contact #2 (the 1st column of STCs on the left), for example, more widely spaced partially independent responses can be discerned for each of the more widely spaced component contacts.

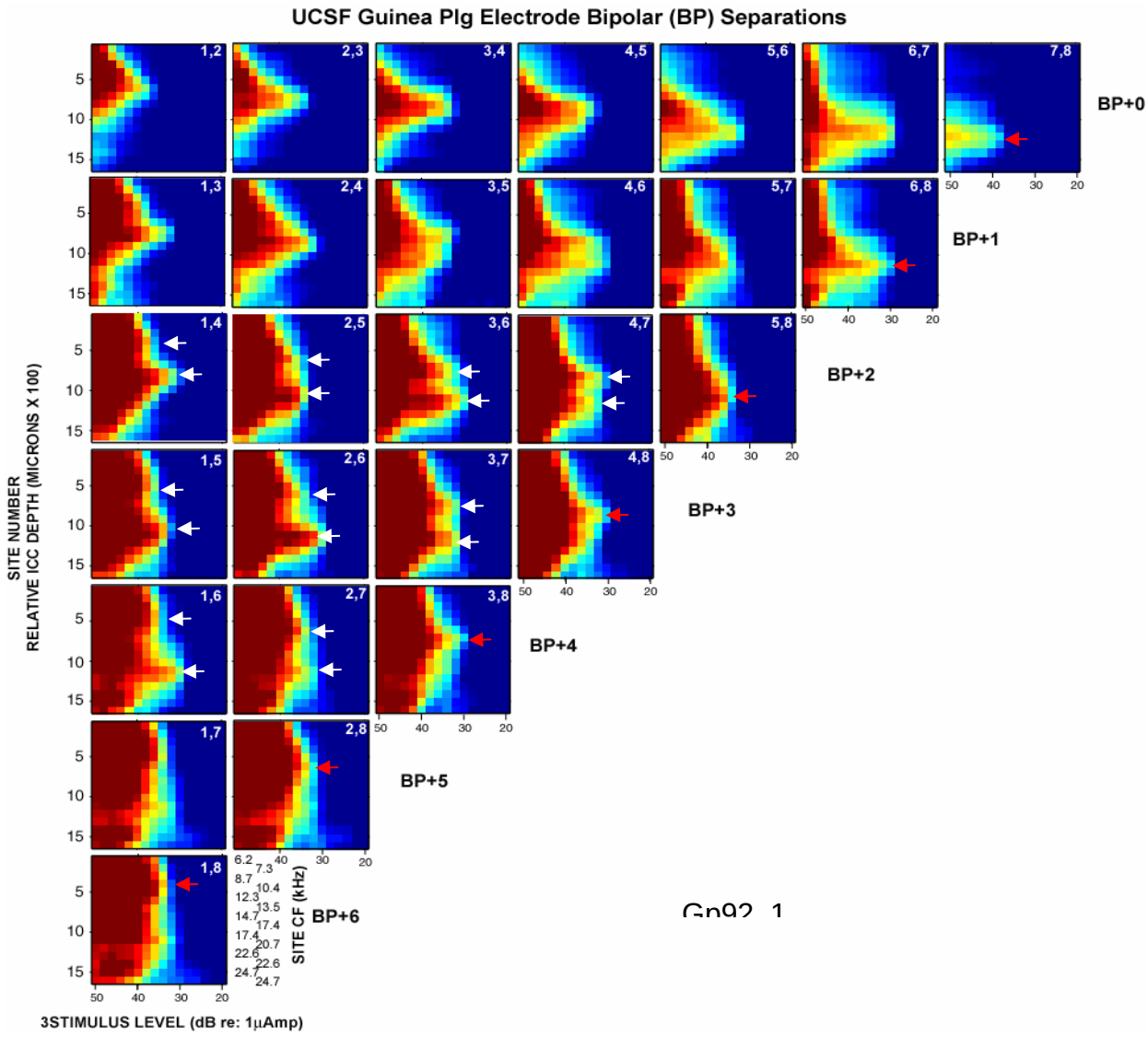

Figure 9. Spatial tuning curves evoked by activation of our guinea pig electrode in successively more widely spaced, bipolar configurations: adjacent bipolar electrodes (BP+0) in the top row to bipolar electrodes separated by 5 electrode contracts (BP+5) in the bottom row. The specific bipolar combinations are indicated in the upper right corner of each STC. The curves are arranged so that the activity patterns evoked by stimulation of the most apical electrode pair is on the far left and those from more basal pairs are placed successively to the right. The characteristic frequencies (CFs) of the recording sites, estimated from acoustic stimulation prior to deafening and implantation, of each recording probe site in this animal is indicated to the right of the bottom row. The white and red arrows indicate interaction peaks that are resolvable in widely spaced bipolar pairs (see text). It should be noted that these data are from a different animal than those presented in the previous figure, but the top row of BP+0 responses in the two figures can be directly compared.

Activation of the more closely space BP+2 contacts (pair 1,4) produce more closely spaced peaks than more widely spaced BP+3 contacts (1,5) and even more widely spaced pairs (1,6). It is interesting that the peak that we associate with contact #1, indicated by the upper arrow in these STCs, moves upward as the separation between contacts increases. We hypothesize that the

movement upward of the peak attributable to this and other contacts in this series may indicate at type of channel interaction, withdrawal of facilitation, as the two constituent contacts become more separated. We further hypothesize that this withdrawal of facilitation can be amplified by using asymmetric biphasic (pseudomonophasic) pulses. We hope to test this hypothesis in the next several experiments. In the discussion above, double peaked STCs were hypothesized to occur when the two constituent contacts are sufficiently widely spaced for their independent responses to be resolved and when they are hypothesized to be equally or nearly equally effective, i.e., have comparable threshold currents. In some cases however, one component electrode may be much less effective, have a much higher threshold, than the other. Activation of such bipolar pairs can produce selective activation of the ICC, but the activity is at a tonotopically inappropriate location – inappropriate in that it does not reflect any contribution of contact 8. For example, in Figure 9, when any electrode is activated in conjunction with contact 8, the resultant activity patterns have peaks that are appropriate for the other electrode (red arrows). This other electrode's activity appears to dominate these STCs, presumably because the thresholds on #8 are so high. These STCs are relatively selective (as compared with their #7 counterparts), and they have activity peaks that are out of sequence with the other STCs in that row. Thus, pair 2,8 has an STC peak appropriate for electrode #2; pair 3,8 has an STC peak appropriate for contact #3, and pair 4,8 has an STC peak appropriate for contact #4. They do not have peaks that could be considered as the addition of two peaks, one attributable to contact #8 and one attributable to the non-8. The red arrows are shifted up consistently the lower frequency of the non-8 contact. This dominance of the responses of contact 8 by all non-8 responses produces STCs that are relatively selective, but tonotopically inappropriate, in that they have activity peak at locations that reflect the expected effects of pairings with such a widely separated contact. Therefore, when widely spaced bipolar pairings are used, selectivity may not be lost or it may be located at unexpected frequency locations. .

Figure 10 gives a statistical summary of effects of electrode configuration on threshold and STC width for 5 experiments. Monopolar threshold tend to be lower than bipolar or tripolar thresholds. Likewise, bipolar stimulation with widely spaced bipoles tends to have lower thresholds than more narrowly spaced bipoles. But none of these differences are statistically significant. This is a surprising result since our experience with other electrodes (e.g., the banded electrode) suggests that these differences should be large. We hypothesize that this lack of difference is due to the close approximation of the contacts to the osseous spiral lamina and to the space filling design of our guinea pig electrode carrier. Analysis of the STCs evoked by the banded electrodes and the VP-ball electrodes in these same animals will test this hypothesis.

The effects of electrode configuration are somewhat clearer. Monopolar configurations are broader than the most narrowly spaced bipoles and tripoles and bipoles are broader than tripoles. But these differences in selectivity are also smaller than we expected and we must await analysis of the banded and VP-ball curves to interpret them. The effects of electrode separation on bipolar (BP+N) STC widths are somewhat clearer as N increases STC width increases, but only the differences between BP+0 and BP+4 are statistically significant. At the widest separations the effects of separation on STC width are complicated by the high thresholds commonly observed on contact #8 and occasionally contact #7. We attribute these relatively high thresholds to poor juxtaposition of these contacts against the osseous spiral lamina caused by the large size of the scala tympani at these locations and the tendency of the electrode cable to pull these most basal intracochlear sites away from the lamina as it exits the bulla (see Figure 6B)..

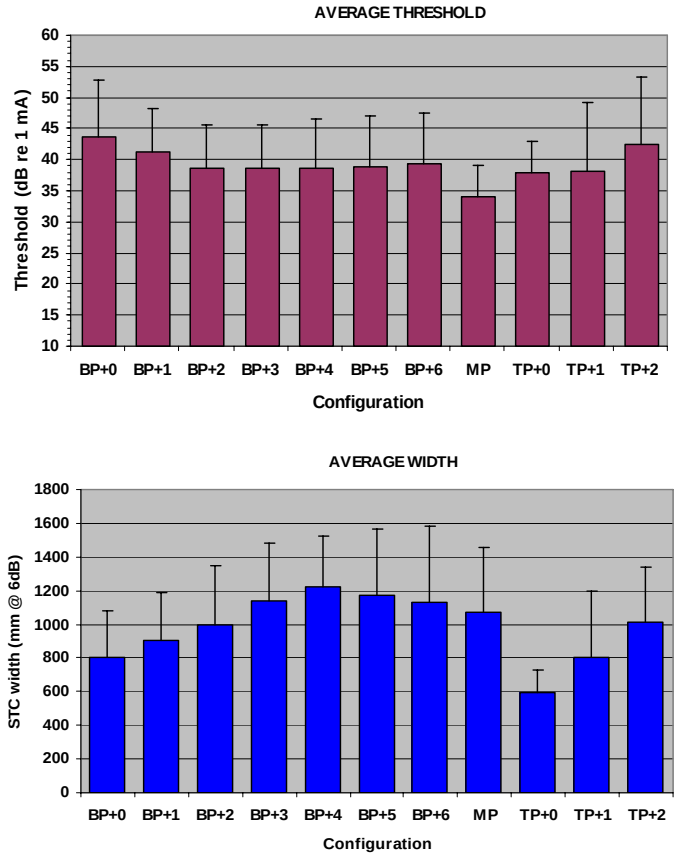

Figure 10. Mean and standard deviations of thresholds and widths (@ +6 dB re threshold) for STCs using guinea pig electrode in the several configurations in 5 guinea pigs.

References

Jeroen J. Briaire and Johan H. M. Frijns, 2000 Field patterns in a 3D tapered spiral model of the electrically stimulated cochlea. Hearing Res. 148:18-20 2000.

Briaire, JJ and JHM Frijns, 1996 Spatial selectivity in a rotationally symmetric model of the electrically stimulated cochlea. Hear Res. 95(1-2):33-48.

Frijns JH, de Snoo SL, Schoonhoven R. 1995 Potential distributions and neural excitation patterns in a rotationally symmetric model of the electrically stimulated cochlea.
Hear Res. 87(1-2):170-86.

Work planned for next quarter

During the next quarter, we plan to continue our experiments using SAM pulse trains. We also plan to begin a series of experiments that will examine responses to SAM acoustic stimuli. The results of these experiments will provide a basis for comparison with responses to SAM electrical pulse trains. We plan to continue our experiments examining interactions between interleaved pulse trains at varying pulse frequencies.
With Don Sinex, we will begin a series of experiments designed to examine responses to specific aspects of electrical stimulation by signals corresponding to speech processed by a cochlear implant processor. We also plan to continue our experiments examining response to other broad-spectrum acoustic stimuli (i.e., noise bands).